Development of an Equivalent Circuit for Batteries Based on a Distributed Impedance Network

Mehdy Khayamy, Adel Nasiri, *Senior Member, IEEE*, and Okezie Okoye

***Abstract*—This paper presents an original equivalent battery model based on a distributed RC circuit. The model virtually includes an infinite number of time constants to reflect the battery behavior, especially during the dynamic stress test. The model has much fewer parameters than the traditional battery model and so reduces the parameterization effort significantly. The self-discharge is inherently implemented in the model as well. The second order partial differential equation of the model is derived and both explicit and numerical solution approaches are introduced to incorporate the model in any simulation environment or analytical response analysis. Incorporating the effect of the state of charge on the parameters of this model is more easily accomplished by changing the trends of the parameters as opposed to each of them individually. The model matches to various battery type and it is validated on a 30 Ah Lithium-Ion battery from 1 C to 8 C discharge pulse current. Furthermore, the results are compared to the classic battery model.**

***Index Terms*—Battery model, electrical equivalent circuit, distributed model, parameter estimation.**

I. Introduction

BATTERIES have existed for a long time, and recently their application are increasing rapidly in a wide range from small toys to electric vehicles all the way to a microgrid peak shaving storage. Battery simulation is a well-known technique to substitute actual battery setup testing to save time and cost during prototyping of battery operation, battery-based power electronic converter control systems, and battery charger design [1], [2].

The battery simulation has been carried using a mathematical model or electrical equivalent circuit (EEC). EEC can help with the real-time diagnostic of the battery-based drive system as well [3]. To reflect the behavior of a battery, EEC usually involves an internal voltage source, a resistor, and one to three series elements of parallel RC branches. The internal voltage represents the majority of the stored energy on the battery and the rest are on the capacitors. The open circuit voltage at the equilibrium state represents state of charge (SOC). The terminal voltage variation to a sudden load change is modeled by the resistor. The RC branches represent various time constants in the battery charge or discharge voltage response [4]–[6].

The battery voltage response seems to be composed of superposition of several time constants. Finding RC parameters depend on the application and the cell chemistry however, a common practice is to define three average time constants for three time intervals for the RC branches. These time intervals depend on the simulation requirement can be second, minute, and hours [2] or tens of seconds, minute, and tens of minutes [7]. These time constants could be selected too short for the battery charger design transient check or relatively long for system level simulation of electric vehicle applications.

Although numerous RC circuits are needed to realistically model a battery from a short to a long time span, the number of RC elements is usually limited by the parameterization effort. Several successful algorithms attempts have been developed to determine the parameters of RC circuits with optimization or analytical methods [7]–[10].

The parameters are also temperature dependent. Finite element method (FEM) [11] and computational fluid dynamics (CFD) [12] are utilized to extract the temperature dependency of the parameters. Analytical methods are also used to determine these dependencies [13], [14] and two-dimensional look-up tables for parameters based on SOC and temperature are suggested [15], [16]. One of the reason that limits the number of RC branches is parameter estimation. The fact that at each SOC, the set of RC parameters that model the behavior of the battery are not unique, makes the parameters versus SOC curve or table to be chaotic. Beside SOC and temperature, internal voltage, resistances and capacitances of the EEC can be influenced by the state of health (SOH) of the battery [17]. Usually, papers which consider SOH, assume the constant temperature [18].

Beside the aforementioned popular classic battery EEC, other EECs have been proposed throughout the years. A parallel parasitic branch with a diode is considered at the terminals of the battery to model the loss charge current which does not increase SOC [19]. A float charge model is proposed in [20] to investigate the effect of the float charge technique. Bode plot technique has been used to assess the battery impedance in the frequency domain and suggest a transfer function [21]. A purely resistive internal impedance but highly nonlinear and current dependent has also been suggested [22]. The application of Warburg element in the battery model [13], [23] and Randle's

Manuscript received July 7, 2019; revised September 29, 2019, December 2, 2019, January 5, 2020, and March 24, 2020; accepted April 19, 2020. Date of publication April 22, 2020; date of current version June 18, 2020. This work was supported by the National Science Foundation under Grant 1650470. The review of this article was coordinated by Prof. M. Preindl. *(Corresponding author: Mehdy Khayamy.)*

Mehdy Khayamy and Adel Nasiri are with College of Engineering and Applied Science, Electrical Engineering Department, University of Wisconsin-Milwaukee, Milwaukee, WI 53211 USA (e-mail: mkhayamy@uwm.edu; nasiri@uwm.edu).

Okezie Okoye is with College of Engineering and Applied Science, Electrical Engineering Department, University of Wisconsin-Milwaukee, Milwaukee, WI 53211 USA, and also with Cummins Inc., Columbus, IN 47201 USA (e-mail: okezieowen@gmail.com).

Digital Object Identifier 10.1109/TVT.2020.2989715

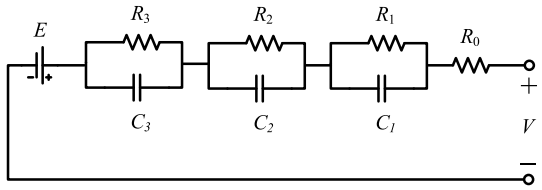

Fig. 1. The conventional electrical equivalent circuit of the battery.

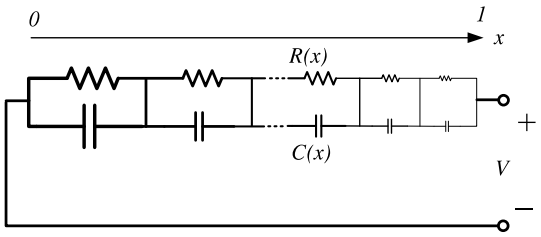

Fig. 2. The suggested equivalent electrical equivalent circuit for the battery.

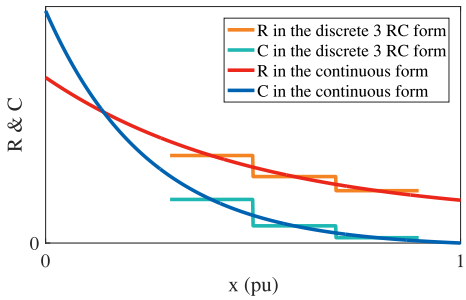

Fig. 3. The concept of discrete and continuous parameter distribution.

equivalent circuit [24] are also investigated. A voltage source connected in parallel with a capacitor through resistors are suggested in [25]. [26] finds an exponential-based function that relates the open circuit voltage and the SOC.

Distribution of the voltage across RC branches for various charge and discharge current is investigated [27]. The separation of the terminal voltage to the internal voltage source and the voltages across RC branches to estimate SOC has been addressed [28].

The results of curve fitting to find the parameters in various operating points is usually does not follow a pattern when the number of RC circuit increases because the solution is not unique. The chaotic dependency of parameters to SOC discourages the simulation of more than three RC branches. Recent research shows at least five RC circuits are required to model an aged battery with a reasonable precision [29].

The accuracy of this simulation depends on the accuracy of the model and the model depends on several parameters that change with operating conditions.

This paper, inspired by the classic EEC, suggests an original model for the battery which overcomes the problems of the existing models. It contains unlimited time constants with very limited parameters. Applying the effect of SOC and temperature on the model is much easier as well because it requires changing the trend of the parameters as opposed to their values. This paper is the first to suggest a distributed impedance network with energy storing component to model the behavior of the battery.

II. Battery Modeling

Depends on the purpose of the study or application, a battery can be modeled with various fidelity. The simplest form is a constant voltage source, E. By adding a resistance, R_0 some of the terminal voltage variation during charge/discharge can be modeled. However, these two simple component do not capture the dynamic time dependent behavior of the battery and that is why RC branches are added to the model. The values of three RC branches are representing three time constants to approximate the voltage response in a certain time interval. The most common EEC of a battery is shown in Fig. 1.

As the battery charge or discharge the terminal voltage varies even at the no current. That was the motivation to have a nonlinear look-up table for the value of E as a function of SOC. One of the complication is the time constants are SOC dependent and there are look-up tables for them as well. Some batteries require 4 or 5 RC branches to properly model the dynamic over a relatively larger time interval. Furthermore, the set of RCs to model the battery at each SOC aren't unique leading to chaotic look-up table trend over the SOC.

The natural progression of the model would be to add more RCs for with various time constant to capture all the dynamics and to smooth the transition of the time constants from one to another and extend the limited time intervals of the model, the concept of unlimited distributed RC branches is introduced. To have uneven RC parameters, the distribution of the parameters are varied over x, which is defined as the per-unit distance between the positive and negative of the battery model. It is considered that x is between 0 and 1.

–Fig. 3 shows the concept of discrete versus continuous of parameter distribution. Fig. 3 is drawn only for the sake of conceptual presentation and not to scale. The three RC systems look like the average of the distributed system which is the combination of several differential RC branches.

Having the three RC branches replaced with the distributed network and looking at the trend of the parameters, it can be concluded that R_0 in the conventional model is a part of the RC network when the relative value of the capacitor to the resistor is negligible. The internal voltage source also can be part of the RC network when the capacitor is huge and the value of resistor is high enough to prevent fast discharge and the only charge loss is due to the battery self-discharge.

The suggested RC network for the battery model is presented in Fig. 2. The distribution of the impedance over x is unique to any battery and called characteristic impedance. The general form of the characteristic impedance can be exponential, (1), polynomial or simply linear. In this paper, the exponential characteristic is adopted. In (1), c_0 and r_0 are the magnitude of the exponential distribution of the resistive and capacitive branches and c_d and r_d are the exponential decay constant.

$$C(x) = c_0 e^{-c_d x} \tag{1a}$$

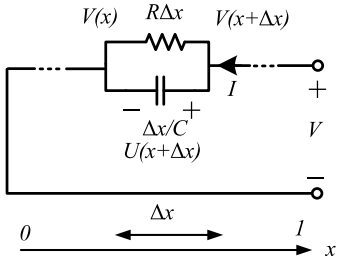

Fig. 4. One element of the characteristic impedance.

$$R(x) = r_0 e^{-r_d x} \tag{1b}$$

III. Model Formulation

Fig. 4 shows one element of the suggested battery model. Elemental voltage, U, is the voltage across one element of the model. Although the current is independent of x throughout the model, the ratio of the elemental capacitor current, I_c, to the resistor current, I_r, is different at any part of the network and the total current is the summation of them as in (2).

$$I = I_r(x) + I_c(x) \tag{2}$$

The current in the resistive path at each element of the network is described by (3).

$$I_r(x) = \frac{V(x+\Delta x) - V(x)}{R\Delta x}$$
$$I_r(x) = \frac{1}{R}\frac{V(x+\Delta x) - V(x)}{\Delta x} \tag{3}$$

The capacitor elemental current is described by (4).

$$I_c(x) = \frac{C}{\Delta x}\frac{\partial\left(V(x+\Delta x) - V(x)\right)}{\partial t}$$
$$I_c(x) = C\frac{\partial}{\partial t}\frac{V(x+\Delta x) - V(x)}{\Delta x} \tag{4}$$

If the length of the elements gets small enough, it results in infinite elements. In other words when Δx gets close to zero, (5) is obtained.

$$\lim_{\Delta x \to 0}\frac{V(x+\Delta x) - V(x)}{\Delta x} = \frac{\partial V}{\partial x} \tag{5}$$

By substituting (5) into (3) and (4) and eventually in (2), the characteristic equation which is a second order partial differential equation that describes the suggested model is obtained as (6).

$$I(t) = \frac{1}{R(x)}\frac{\partial V(x,t)}{\partial x} + C(x)\frac{\partial^2 V(x,t)}{\partial t \partial x} \tag{6}$$

IV. The Solution to the Characteristic Equation

The explicit solution for equation (6) for exponential distribution of the resistance and capacitance, as well as a numerical solution to an arbitrary distribution, are provided. For the explicit solution the current is considered to be constant and for the numerical analysis, the current can have any arbitrary waveform. As Δx tends to zero, the elemental voltage, U becomes the partial derivative of the voltage with respect to x, (7).

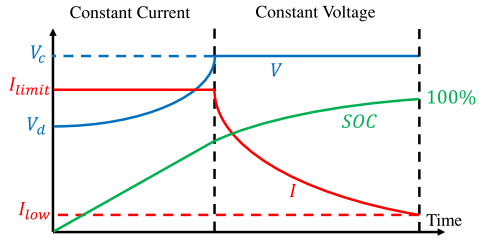

Fig. 5. The typical charge profile.

$$U(x,t) = \frac{\partial V(x,t)}{\partial x} \tag{7}$$

Considering (7), equation (6) can be simplified to (8) which is a first order ODE in time at any x.

$$I(t) = \frac{1}{R(x)}U(x,t) + C(x)\frac{\partial U(x,t)}{\partial t} \tag{8}$$

A. Initial Voltage Distribution of a Fully Charged Battery

The initial distribution of the voltage across x is necessary for both of the solutions. Fig. 5 shows a typical charge profile with the constant current and constant voltage regions. The charge process starts when SOC is low enough and the battery voltage is at the discharged voltage, V_d. The battery is being charged with the maximum limit current until the voltage reaches the charged voltage, V_c. To keep the voltage constant at V_c, the current needs to reduce. The charging cycle typically ends when the charging current gets lower than a minimum current, I_{low} [1].

Considering the battery model as a network of RC branches, when the system is fully charged, the whole current passes from the resistive branch in Fig. 2. In the case of the battery model, this current is close to zero. Therefore, the voltage across each element has the same shape of the resistance of that element and the total voltage scaled to have the accumulated value V_c. The initial voltage distribution across x is described in (9).

$$U(x,0) = U_{0c} = \frac{V_c}{\int_0^1 R(x)dx}R(x) \tag{9}$$

For the exponential distribution it is (10).

$$U_{0c}(x) = \frac{V_c r_d}{1 - e^{-r_d}}e^{-r_d x} \tag{10}$$

Hence, the initial voltage distribution is (11).

$$V_{0c}(x) = \int U_{0c}dx = \frac{-V_c}{1 - e^{-r_d}}e^{-r_d x} + k \tag{11}$$

parameter $k = V(1,0)$ which is the integral constant can be found with the constraint that $V_{0c}(1) = V_c$ as

$$k = V_c + \frac{V_c}{1 - e^{-r_d}}e^{-r_d} \tag{12}$$

The initial voltage distribution is (13):

$$V_{0c}(x) = V_c\left(1 - \frac{e^{-r_d x} - e^{-r_d}}{1 - e^{-r_d}}\right) \tag{13}$$

Since the voltage, V, at each point is measured with respect to the negative port of the battery model, the initial voltage is zero at $x = 0$ and is V_c at $x = 1$. Halving another battery cell with a different voltage rating, only V_c needs to be changed in (13).

B. The Explicit Solution

The explicit solution is insightful about the behavior of the battery and the determination of its parameters. Equation (8) in Laplace domain is (14) which requires the initial voltage distribution over x.

$$\frac{1}{s}I = \frac{1}{R}U + C\left(sU - U_{0c}\right) \tag{14}$$

Substituting (10) into (14) and arranging it in term of U, results in (15).

$$U = \frac{\frac{1}{c_0 e^{-c_d x}}}{s + \frac{1}{c_0 r_0 e^{-(c_d + r_d)x}}} \left(\frac{1}{s}I + V_c \frac{c_0 r_d}{1 - e^{-r_d}} e^{-(c_d + r_d)x}\right) \tag{15}$$

By taking inverse Laplace, U can be converted back to the time domain as (16).

$$U = \left(V_c \frac{r_d}{1 - e^{-r_d}} - r_0 I\right) e^{-r_d x} e^{\frac{-t}{c_0 r_0} e^{(c_d + r_d)x}} + r_0 I e^{-r_d x} \tag{16}$$

The term $\tau(x) = c_0 r_0 e^{-(c_d + r_d)x}$ is the time constant of each element. To find the voltage, integral of U needs to be calculated. The challenging term is defined as J in (17). A new variable of z is defined to simplify the integral and rewrite J in term z instead of x.

$$J = \int_0^1 e^{-r_d x} e^{\frac{-t}{c_0 r_0} e^{(c_d + r_d)x}} dx \tag{17}$$

$$z = \frac{1}{c_0 r_0} e^{(c_d + r_d)x} \tag{18}$$

$$e^{-r_d x} = \left(\frac{1}{c_0 r_0}\right)^{\frac{r_d}{r_d + c_d}} \times z^{\frac{-r_d}{r_d + c_d}} \tag{19}$$

$$dx = \frac{1}{(r_d + c_d)z} dz \tag{20}$$

$$J = \frac{1}{r_d + c_d} \left(\frac{1}{c_0 r_0}\right)^{\frac{r_d}{r_d + c_d}} \times \int_{\frac{1}{c_0 r_0}}^{\frac{1}{c_0 r_0} e^{(c_d + r_d)}} z^{-\left(\frac{r_d}{r_d + c_d} + 1\right)} e^{-tz} dz \tag{21}$$

The integral in terms of z has a solution in term of $Ei(a, x)$ which is an exponential integral function with order a (22).

$$\int z^{-(a+1)} e^{-tz} dz = -z^{-a} Ei\left(a + 1, tz\right) \tag{22}$$

Therefore J is (23).

$$J(t) = \frac{1}{c_d + r_d} Ei\left(\frac{r_d}{c_d + r_d} + 1, \frac{t}{c_0 r_0}\right) - \frac{1}{c_d + r_d} e^{-r_d} Ei\left(\frac{r_d}{c_d + r_d} + 1, \frac{t}{c_0 r_0} e(c_d + r_d)\right) \tag{23}$$

Having J, the battery voltage is determined by integrating U in (16) as (25).

$$V_b(t) = \int_0^1 U(x, t) dx \tag{24}$$

$$V_b(t) = \left(V_c \frac{r_d}{1 - e^{-r_d}} - r_0 I\right) J(t) + \frac{r_0}{r_d} I(1 - e^{-r_d}) \tag{25}$$

In summary, the battery terminal voltage can be found from (26)

$$V_b(t) = \int_0^1 \int_0^{t_0} \left(\frac{1}{C(x)} \left(I(t) - \frac{1}{R(x)} U(x, t)\right)\right) dt dx \tag{26}$$

C. The Numerical Solution

The numerical solution provides flexibility in choosing any parameter distribution and current waveform. To numerically solve equation (6), time step and space step need to be chosen to discretize time interval, Δt, and space interval, Δx. Δt depends on the total simulation time and kind of needed transient response. The higher the accuracy, lower Δx, the higher computational load will be. In this manuscript, for the sake of the fine figures $\Delta x = 0.01$ is chosen which results in a great precision and 100 RC branches.

For the standard trapezoidal numerical integration, equation (8) for any x_i the element voltage can be found as (27).

$$U(x_i, t_{i+1}) = \frac{\Delta t}{C(x_i)} \left(I(t_i) - \frac{1}{R(x_i)} U(x_i, t_i)\right) \tag{27}$$

The terminal voltage is (28).

$$V(x_{i+1}, t_{i+1}) = \Delta x U(x_i, t_{i+1}) + V(x_i, t_{i+1}) \tag{28}$$

The voltage of each RC element needs to be calculated using eq. (27) and added together by eq. (28). Selection of the Δx depends on the application. A higher Δx can be selected for faster computation or a lower Δx for better accuracy. It is a trade off between the accuracy and computation. The suggested EEC enables us to arbitrary increase the accuracy, if needed, without being worry about a huge set of parameter estimation.

D. Computation Requirement

When the battery current waveform is predefined or constant, an explicit closed-form solution is preferable because of the minimal computational requirement. If the battery current waveform is unpredictable the numerical solution can be applied.

The computational requirement of the suggested EEC and the classic battery model is discussed as follows. For a classic battery model, the terminal voltage is the sum of the internal voltage, three RC branches, and a resistive voltage drop which makes it 5 series components. The computation is comparable to the suggested EEC with $\Delta x = 0.2$. However, it requires several high precision look-up tables to store the values of E, R_0, and

each of the RCs. Usually, the resolution is 50 value, one for each 2% SOC.

A Δx lower than 0.2 can be selected for better accuracy. It is a trade-off between the accuracy and computational requirement. The suggested EEC enables us to arbitrary increase the accuracy, if needed, without worrying about a huge set of parameter estimation. $\Delta x = 0.1$ means twice the classic model computational time but it does not require look-up table memory fetching.

V. The Characteristic Impedance

The nature of the characteristic impedance for a Lithium-Ion battery is discussed in this chapter. The parameters of the characteristic impedance are unique for each battery.

A. The Effect of SOC

The distribution of the parameters as a function of SOC in the conventional battery model is usually chaotic [23], [27] and the more RC elements, the more chaotic it would be. One of the main reason is the curve fitting algorithms or the optimization methods to find the parameters. Since the solution is not unique a battery at a certain SOC can be defined by higher τ_1 and lower τ_2 or the other way around even in the case of two RC branches. These multiple solutions cause relatively sharp sudden variations in the trend of parameters versus SOC. On the other hand, one of the restrictions of having more RC branches is finding the parameters in a meaningful manner with a coherent trend.

Applying the SOC dependency to the suggested model is much easier. Since the capacitor represents the stored energy in the battery, it can not be changed. The resistance on the other hand can be increased. r_0 in eq. (29) is the magnitude of the resistance distribution when the battery is fully charged. r_0 needs to be adjusted as the battery loses charge. A simple quadratic resistance increase is suggested here as (29).

$$r_0(DOD) = r_0\left(1 + (k_1 DOD + k_2 DOD^2)\right) \tag{29}$$

$$DOD = 1 - SOC \tag{30}$$

where DOD is depth of discharge. When the battery is fully charged $(SOC = 1, DOD = 0)$, $r_0(0) = r_0$. $r_0(DOD)$ increases as DOD increases from 0 to 1 and the rate of change is defined by k_1 which multiplies by DOD and k_2 which is the coefficient of DOD squared.

B. Matching the Parameters

A cylindrical lithium-ion cell, VL30PFe, [30], is used to adopt the model. The battery is 30 A 1 C with the voltage range of 3.1 to 3.5 V. To find the parameters of the characteristic impedance of (1), MATLAB Simulink Design Optimization has been used to find the parameters of the model to match the actual hardware data.

Table I shows the parameters of the impedance distribution described in (1). Fig. 6 shows the trend of the characteristic impedance for a Li-ion battery. Fig. 6(a) shows the value of resistor and capacitor of the characteristic impedance versus x. The trajectory of the characteristic impedance is shown in Fig. 6(c) as well.

TABLE I
Parameter of the Characteristic Impedance

Parameters	Value
c_0	3.502×10^{12}
c_d	31.28
r_0	5.42×10^{6}
r_d	28.29
k_1	0.0419
k_2	2.505

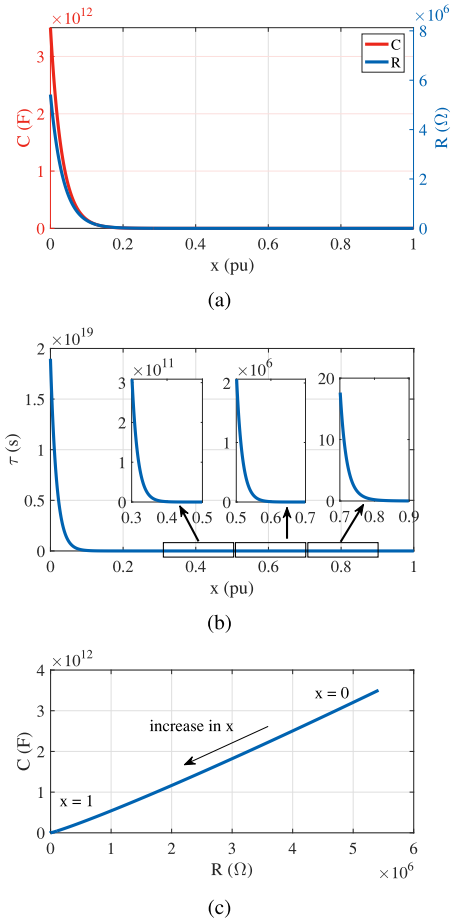

Fig. 6. Characteristic Impedance: (a) resistance and capacitance distribution; (a) time constant distribution; and (c) impedance trajectory of capacitor versus resistance.

VI. Interpretation of the Model

Fig. 7(a) is the voltage distribution, U, during a constant current charge and discharge when the battery is being charged with a constant current.

Both resistance and capacitance at the beginning of the model, close to the terminal or when x tends to 1, are very low. The capacitors are being fully charged fast and the voltage across them at the steady-state is simply the current multiplied by the resistance which is negligible. The deep capacitance, when x is close to 0, is very high and the current does not increase the voltage by much. The voltage when $x \approx 0.5$, however, increases significantly by the charge current as it is shown in Fig. 7(a),

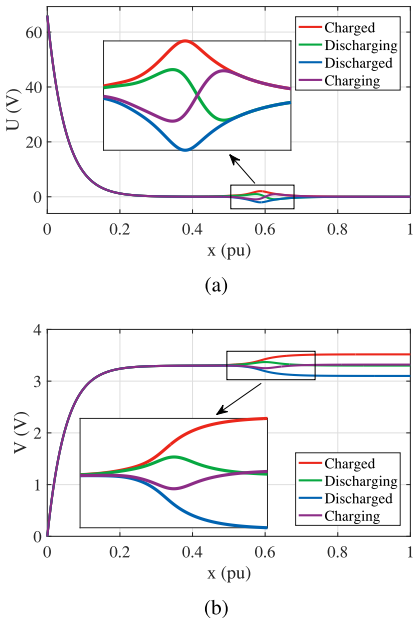

Fig. 7. Charged and Discharged voltage profile by constant rated current: (a) elemental voltage; and (b) accumulated voltage.

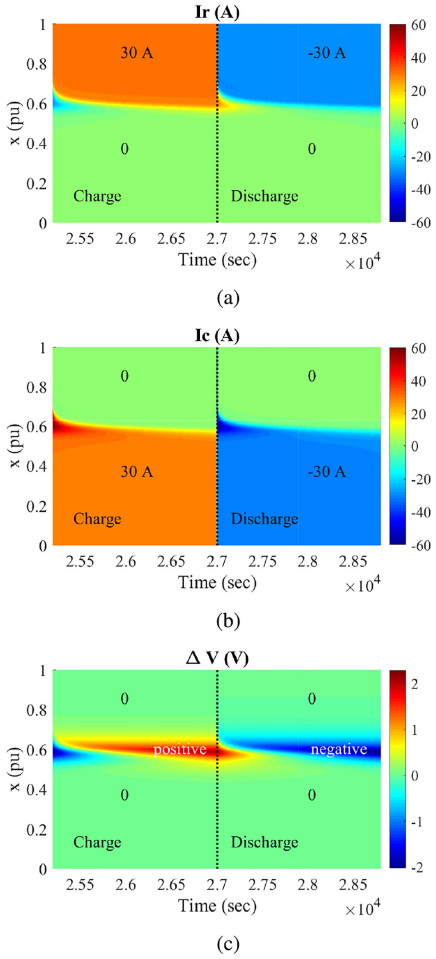

Fig. 8. Voltage and current during charge and discharge at constant current: (a) resistive branch current; (b) capacitive branch current; and (c) voltage difference with a gradual fully charged profile.

$Charged$ curve. Similarly, the constant current discharge current can cause a negative voltage in the middle range of the model, $Discharged$. The transition from charged to discharged, $Discharging$, and discharged to charged, $Charging$, are also shown in Fig. 7(a). Fig. 7(b) shows the accumulated voltage across the model, V, as (24).

To illustrate how voltage and current are changing in the model, Fig. 8 is shown. The vertical axis is x with the distribution of $R(x)$ and $C(x)$ shown in Fig. 6(a). Figs. 8(a), 8(b) are the share of current in the resistor and capacitor branches respectively. For the low capacitance part of the model, when x is close to 1, the 30 A charging current almost entirely passed from the resistive path of the model and almost nothing from the capacitive path because the capacitance are so small they get completely charged almost immediately (Figs. 8(a), 8(b) upper left corners). For the high capacitance part of the model, when x is close to 0, almost all of the current passes from the capacitive branch because they take a long time to charge and their voltage doesn't change much as the current passes leaving almost no current from the resistive paths (Figs. 8(a), 8(b) lower left corners). A similar explanation applies to the discharge on the right hand side of the figures.

To show the voltage variation during charge or discharge, Fig. 8(c) shows the difference between the voltage distribution during equilibrium state and the voltage distribution when the battery is getting charged or discharged with a constant current. The change of the voltage on the low impdedance side of the model is negligible and the voltage across the high capacitance elements doesn't change much by current. The only section that changes on a short term with a charge or dischage current is the middle part. It is shown on Fig. 7 as well.

One of the observation is that the sudden reversal of the current from charging to discharging or the other way around causes twice the current in the capacitor branches.

Considering the typical charge curve (Fig. 5), as soon as the voltage increases in the middle of the x the accumulated voltage, V, reaches to the charged voltage and after that the current needs to decreases to reduce the inflated voltage in the middle and provide more time for the deeper and higher capacitor area of the model to charge. The voltage of a battery getting charged and discharged for a long time with a minimal current is shown in Fig. 9.

Fig. 5 shows the charge process with CC and CV regions. The corresponding voltage at several stages of charge is shown in Fig. 10 as well as Fig. 11. Fig. 11 illustrate how the suggested model explains the concept of deep charging and how the voltage distribution changes as the battery is getting charged in the constant voltage region. The deeper capacitors, $C(x)$ when x is closer to 0, are getting charged and since they have a higher capacitance, with the same voltage the battery keeps a higher energy. The explanation of sub-figures in Fig. 11 are similar to

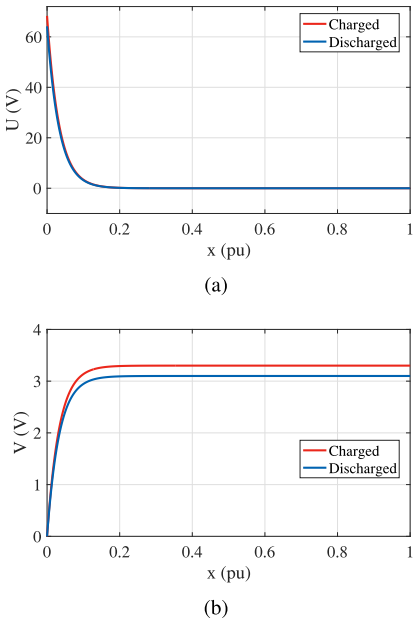

Fig. 9. Charged and Discharged voltage profile when charged and discharged for a very long time by very small current: (a) elemental voltage; and (b) accumulated voltage.

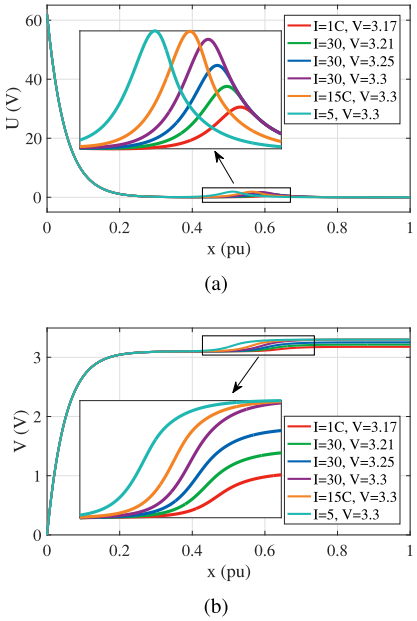

Fig. 10. The profile of voltage in a gradual charging process including CC and CV: (a) elemental voltage; and (b) accumulated voltage.

Fig. 8. Over the CV region, to keep the voltage constant, the charging current is getting lower and lower as time passes.

VII. The System Response to the Pulse Load

Two pulse loads have been applied to the model as well as actual battery cell at 1 C which is 30 A and 8 C which is 240 A. The battery current and voltage in addition to the model terminal

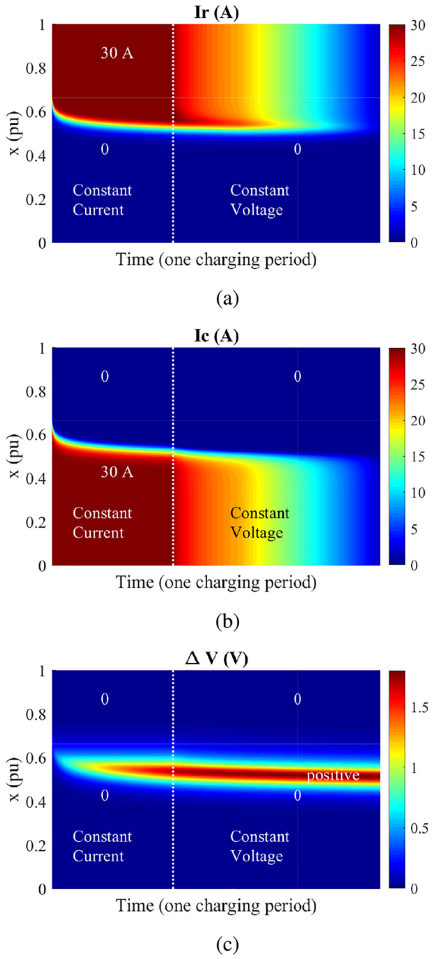

Fig. 11. Voltage and current during a charge cycle including the constant current and the constant voltage: (a) resistive branch current; (b) capacitive branch current; and (c) voltage difference with a gradual fully charged profile.

TABLE II
Comparison Metrics for the Traditional and Distributed EECs

	1C pulses		8C pulses	
	traditional	Distributed	traditional	Distributed
RMSE	0.01802	0.0052	0.0234	0.0051
Average Error	0.0271 %	0.0102 %	0.0414 %	0.0240 %

voltage are shown in Figs. 12 and 13 which shows the model response matches the actual voltage of the battery cell.

Figs. 12(c) and 13(c) show the error percentage between the terminal and model voltages. Table II shows the root-mean-squared error (RMSE) and absolute average error between the actual and modeled voltages for both load profile for the clasic and the suggested distributed model. The average of error for 1 C is very low as shown in Fig. 12(c) and Table II. For 8 C the average error is still very low but there is a difference for a few sample times between the drastic voltage drop of the model and the cell for a 240 A load. It is worth mentioning that the voltage of the battery is dropped to 2.7 V in Fig. 13(b) which is lower than the minimum steady-state battery voltage at 0 SOC but it doesn't mean the battery SOC is lower than 0% and as soon as

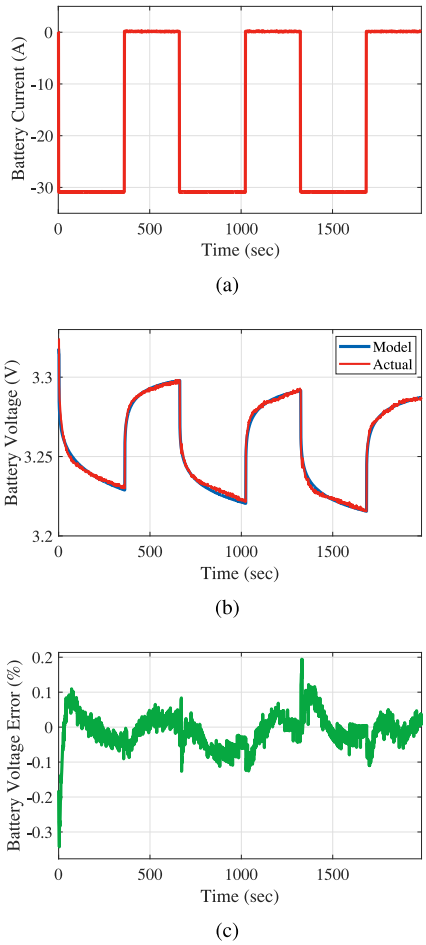

Fig. 12. The voltage and current of the battery and model during 1 C pulses: (a) current; (b) voltage; and (c) voltage difference.

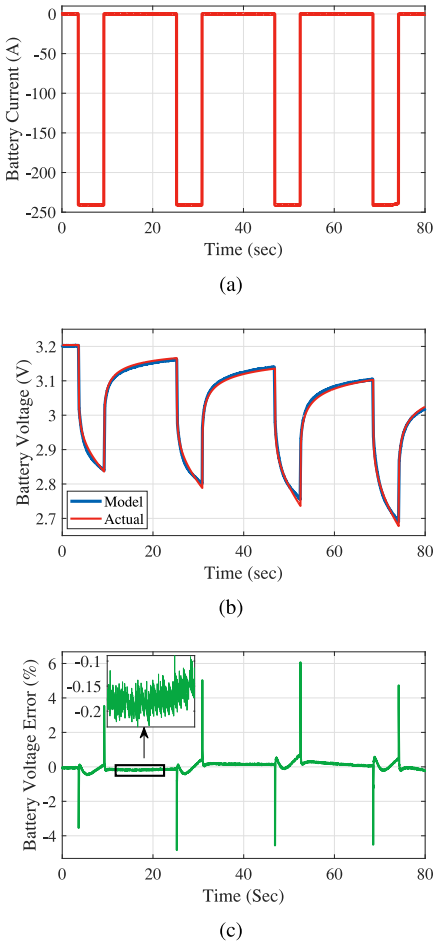

Fig. 13. The voltage and current of the battery and model during 8 C pulse: (a) current; (b) voltage; and (c) voltage difference.

the high current pulse load turns off for an enough long time, the voltage recovers to a value in the range of 3.1–3.5 V. A 16 bit analog to digital converter board is used for this project.

A traditional EEC with 3-RC branches is modeled as well and the parameters are found with the same MATLAB Simulink Design Optimization which we used for the suggested model. The model response matches the actual voltage with a great accuracy and the scaled parameters are shown in Fig. 14 which shows the chaotic variation of various parameters with respect to SOC.

Remark 1: Although the method is computationally more demanding compared to the traditional EEC, it does not need heavy look-up tables to store the value of various traditional model parameters versus SOC. Since the values of traditional EEC parameters do not have a predictable pattern versus SOC, an accurate SOC estimation and high-resolution parameters versus SOC data are needed to rely on the model to predict the behavior of the battery. Parameter estimation versus SOC can be done at each 2% SOC [29]. If a more precise model is required, more parameter estimation and heavier loop-up tables are needed. The suggested EEC is not sensitive to SOC.

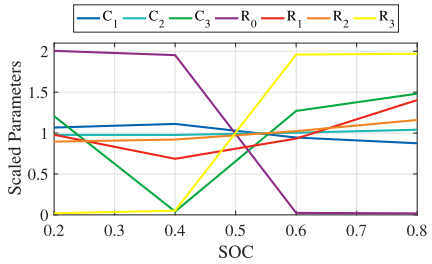

Fig. 14. Scaled parameters for EEC with 3 RC branches.

Remark 2: To incorporate the effect of the temperature into the model, scaling up r_0 and c_0 rather than c_d and r_d might be enough. The relation between r_0 and c_0 and temperature needs to be found.

Remark 3: Aged batteries are usually distinguished from a brand new batteries by their reduced capacity and excessive heating during charge or discharge. Since the suggested model does not have an ideal internal voltage source, and it is comprised of capacitors and resistors, it seems like a perfect opportunity to incorporate the SOH.

There are two exponential curve describing the capacitance and resistance distribution for the suggested model. The effect

of the battery usage aging and calendar aging might on the main parameters of c_0, r_0, c_d, and r_d needs to be investigated.

VIII. Conclusion

A realistic, high precision electrical equivalent circuit for the battery is suggested in this paper. The model consists of infinite number of time constants to adapt the dynamic response of the battery model to any battery terminal voltage responses. Exponential parameter distribution is chosen for the elemental RC branches and the equation describing the distributed model has been derived. Instead of the internal voltage, three RC branches parameters and series resistance look up tables versus SOC which are common for the classic EEC, the model requires the resistance and capacitance distribution functions to incorporate all of the aforementioned roles. Both of analytic and numerical solutions of the model were derived. The model naturally incorporates self-discharge. The model predicts the dynamics of the battery voltage response by including distributed time constants. Despite the vast range of time constant, the model requires few parameters and hence, it is easier to find the parameters with a coherent trend.

Both of the classic EEC and the suggested distributed EEC has been adapted to a cylindrical lithium-ion cell and 1 C and 8 C load step pulses have been applied to the system. It is shown the distributed model can track the dynamic response of the battery with a higher accuracy thanks to its infinite time constants.

Future work could focus on incorporating the effect of the temperature as well as aging on the parameter distribution function.

Acknowledgment

Any opinions, findings, and conclusions or recommendations expressed in this material are those of the author(s) and do not necessarily reflect the views of the National Science Foundation.

References

[1] J. F. Wu, C. L. Wei, and Y. Z. Juang, "A monolithic high-voltage Li-ion battery charger with sharp mode transition and partial current control technique," *IEEE Trans. Circuits Syst. I: Regular Papers*, vol. 65, no. 9, pp. 3099–3109, Sep. 2018.

[2] Y. Cao, R. C. Kroeze, and P. T. Krein, "Multi-timescale parametric electrical battery model for use in dynamic electric vehicle simulations," *IEEE Trans. Transp. Electrific.*, vol. 2, no. 4, pp. 432–442, Dec. 2016.

[3] A. Scacchioli, G. Rizzoni, M. A. Salman, W. Li, S. Onori, and X. Zhang, "Model-based diagnosis of an automotive electric power generation and storage system," *IEEE Trans. Sys., Man, Cybern.: Syst.*, vol. 44, no. 1, pp. 72–85, Jan. 2014.

[4] Z. M. Salameh, M. A. Casacca, and W. A. Lynch, "A mathematical model for lead-acid batteries," *IEEE Trans. Energy Convers.*, vol. 7, no. 1, pp. 93–98, Mar. 1992.

[5] B. Schweighofer, K. M. Raab, and G. Brasseur, "Modeling of high power automotive batteries by the use of an automated test system," *IEEE Trans. Instrum. Meas.*, vol. 52, no. 4, pp. 1087–1091, Aug. 2003.

[6] M. Einhorn, F. V. Conte, C. Kral, and J. Fleig, "Comparison, selection, and parameterization of electrical battery models for automotive applications," *IEEE Trans. Power Electron.*, vol. 28, no. 3, pp. 1429–1437, Mar. 2013.

[7] A. Hentunen, T. Lehmuspelto, and J. Suomela, "Time-domain parameter extraction method for thvenin-equivalent circuit battery models," *IEEE Trans. Energy Convers.*, vol. 29, no. 3, pp. 558–566, Sep. 2014.

[8] T. Hu, B. Zanchi, and J. Zhao, "Simple analytical method for determining parameters of discharging batteries," *IEEE Trans. Energy Convers.*, vol. 26, no. 3, pp. 787–798, Sep. 2011.

[9] Z. Yu, L. Xiao, H. Li, X. Zhu, and R. Huai, "Model parameter identification for lithium batteries using the coevolutionary particle swarm optimization method," *IEEE Trans. Ind. Electron.*, vol. 64, no. 7, pp. 5690–5700, Jul. 2017.

[10] D. Dvorak, T. Bäuml, A. Holzinger, and H. Popp, "A comprehensive algorithm for estimating Lithium-ion battery parameters from measurements," *IEEE Trans. Sustain. Energy*, vol. 9, no. 2, pp. 771–779, Apr. 2018.

[11] W. Renhart, C. Magele, and B. Schweighofer, "Fem-based thermal analysis of NiMH batteries for hybrid vehicles," *IEEE Trans. Magn.*, vol. 44, no. 6, pp. 802–805, Jun. 2008.

[12] X. Hu, S. Lin, S. Stanton, and W. Lian, "A foster network thermal model for hev/ev battery modeling," *IEEE Trans. Ind. Appl.*, vol. 47, no. 4, pp. 1692–1699, Jul. 2011.

[13] M. Greenleaf, O. Dalchand, H. Li, and J. P. Zheng, "A temperature-dependent study of sealed lead-acid batteries using physical equivalent circuit modeling with impedance spectra derived high current/power correction," *IEEE Trans. Sustain. Energy*, vol. 6, no. 2, pp. 380–387, Apr. 2015.

[14] R. R. Richardson and D. A. Howey, "Sensorless battery internal temperature estimation using a Kalman filter with impedance measurement," *IEEE Trans. Sustain. Energy*, vol. 6, no. 4, pp. 1190–1199, Oct. 2015.

[15] K. Murashko, J. Pyrhönen, and L. Laurila, "Three-dimensional thermal model of a lithium ion battery for hybrid mobile working machines: Determination of the model parameters in a pouch cell," *IEEE Trans. Energy Convers.*, vol. 28, no. 2, pp. 335–343, Jun. 2013.

[16] J. Jaguemont, A. Nikolian, N. Omar, S. Goutam, J. V. Mierlo, and P. V. den Bossche, "Development of a two-dimensional-thermal model of three battery chemistries," *IEEE Trans. Energy Convers.*, vol. 32, no. 4, pp. 1447–1455, Dec. 2017.

[17] H. F. Yuan and L. R. Dung, "Offline state-of-health estimation for high-power lithium-ion batteries using three-point impedance extraction method," *IEEE Trans. Veh. Technol.*, vol. 66, no. 3, pp. 2019–2032, March 2017.

[18] J. Kim and B. H. Cho, "State-of-charge estimation and state-of-health prediction of a li-ion degraded battery based on an EKF combined with a per-unit system," *IEEE Trans. Veh. Technol.*, vol. 60, no. 9, pp. 4249–4260, Nov. 2011.

[19] M. Ceraolo, "New dynamical models of lead-acid batteries," *IEEE Trans. Power Syst.*, vol. 15, no. 4, pp. 1184–1190, Nov. 2000.

[20] P. M. Hunter and A. H. Anbuky, "Vrla battery virtual reference electrode: Battery float charge analysis," *IEEE Trans. Energy Convers.*, vol. 23, no. 3, pp. 879–886, Sep. 2008.

[21] J. Jang and J. Yoo, "Equivalent circuit evaluation method of lithium polymer battery using bode plot and numerical analysis," *IEEE Trans. Energy Convers.*, vol. 26, no. 1, pp. 290–298, Mar. 2011.

[22] S. X. Chen, H. B. Gooi, N. Xia, and M. Q. Wang, "Modelling of lithium-ion battery for online energy management systems," *IET Elect. Syst. Transp.*, vol. 2, no. 4, pp. 202–210, Dec. 2012.

[23] M. Greenleaf, H. Li, and J. P. Zheng, "Modeling of li_xfepo_4 cathode li-ion batteries using linear electrical circuit model," *IEEE Trans. Sustain. Energy*, vol. 4, no. 4, pp. 1065–1070, Oct. 2013.

[24] C. R. Lashway and O. A. Mohammed, "Adaptive battery management and parameter estimation through physics-based modeling and experimental verification," *IEEE Trans. Transp. Electrific.*, vol. 2, no. 4, pp. 454–464, Dec. 2016.

[25] C. Zhao, H. Yin, Z. Yang, and C. Ma, "Equivalent series resistance-based energy loss analysis of a battery semiactive hybrid energy storage system," *IEEE Trans. Energy Convers.*, vol. 30, no. 3, pp. 1081–1091, Sep. 2015.

[26] T. Mesbahi, N. Rizoug, F. Khenfri, P. Bartholomeüs, and P. L. Moigne, "Dynamical modelling and emulation of Li-ion batteries; Supercapacitors hybrid power supply for electric vehicle applications," *IET Elect. Syst. Transp.*, vol. 7, no. 2, pp. 161–169, 2017.

[27] M. Bahramipanah, D. Torregrossa, R. Cherkaoui, and M. Paolone, "Enhanced equivalent electrical circuit model of lithium-based batteries accounting for charge redistribution, state-of-health, and temperature effects," *IEEE Trans. Transp. Electrific.*, vol. 3, no. 3, pp. 589–599, Sep. 2017.

[28] J. Yang, B. Xia, Y. Shang, W. Huang, and C. C. Mi, "Adaptive state-of-charge estimation based on a split battery model for electric vehicle applications," *IEEE Trans. Veh. Technol.*, vol. 66, no. 12, pp. 10 889–10 898, Dec. 2017.

[29] R. Ahmed *et al.*, "Model-based parameter identification of healthy and aged Li-ion batteries for electric vehicle applications," *SAE Int. J. Alternative Powertrains*, vol. 4, no. 2, pp. 233–247, 2015.

[30] "Saft Batteries," [Online]. Available: http://www.houseofbatteries.com/documents/LithiumIonAdvantage.pdf, Accessed Sep. 25, 2019.

Mehdy Khayamy was born in Ahvaz, Iran. He received the B.S.c. degree in electrical engineering from the Chamran University of Ahvaz, Iran, in 2004, The M.Sc. degree in electrical engineering from the University of Tehran of Tehran, Iran, in 2008, and the Ph.D. degree in electrical engineering from Tennessee Technological University, Cookeville, Tennessee, in 2017. His master's and doctoral research are focused on power electronics and the development of control algorithms for control of electric machines and control of control power electronic converters for solar and wind renewable energy systems and battery applications. He worked for MAPNA Group company from 2010 to 2012 as the Test and Commissioning Engineer for the generator field rectifier, static excitation system, and generator/turbine initial start-up, static frequency converter. He published a book on the application of MATLAB in mathematics back in Iran. He also worked as a Postdoc Researcher at the University of Wisconsin Milwaukee from 2017 to 2018 and he is continuing his collaboration with the university to the present day. Currently, he is a Lead Power Conversion Engineer at the R&D division of Eaton Corporation, Menomonee Falls, Wisconsin.

During his postdoc he focused on the dual active bridges and modeling of batteries and during his R&D job he worked on arc-less voltage regulator by using power electronics as well as medium voltage extreme fast charger for electric vehicles.

Adel Nasiri (Senior Member, IEEE) received B.S. and M.S. degrees from the Sharif University of Technology, Tehran, Iran, in 1996 and 1998, respectively, and the Ph.D. degree from the Illinois Institute of Technology, Chicago, Illinois, in 2004, all in electrical engineering. He worked for Moshanir Power Engineering Company, from 1998 to 2001. He also worked for Health Technologies, Inc., Daytona Beach, Florida, from 2004 to 2005. He presently a Professor and Director of Center for Sustainable Electrical Energy Systems, College of Engineering and Applied Sciences, University of WisconsinMilwaukee. His research interests are renewable energy interface, energy storage, and microgrids. Dr. Nasiri has published numerous technical journal and conference papers on related topics. He also holds seven patent disclosures. He is a Co-Author of two books and several book chapters. Dr. Nasiri is currently an Associate Editor of IEEE TRANSACTIONS ON INDUSTRY APPLICATIONS, an Editor of *Power Components and Systems*, and Associate Editor of the *International Journal of Power Electronics* and was an Editor of IEEE TRANSACTIONS ON SMART GRID (2013–2019). He was the General Chair of 2012 IEEE Symposium on Sensorless Electric Drives, 2014 International Conference on Renewable Energy Research and Applications (ICRERA 2014), and 2014 IEEE Power Electronics and Machines for Wind and Water Applications (PEMWA 2014).

Okezie Okoye received the bachelor's degree in electronic and electrical engineering from Obafemi Awolowo University, Ife, Nigeria, in 2013, and the master's degree in electrical engineering from Tennessee Technological University, Cookeville, TN, USA, in May 2017. During his master's study, his research focused on adaptive control of battery chargers, electric machine drives and renewable energy systems. This research work has produced more than five journal and conference publications. Mr. Okoye currently works as an Electronic Controls Engineer with Cummins Inc., Columbus, IN, USA, where he works on developing and integrating controls software for off-road vehicles.